STRUCTURAL CONTROL AND HEALTH MONITORING
Struct. Control Health Monit. 2006; **13**:561–569
Published online 9 December 2005 in Wiley InterScience (www.interscience.wiley.com). DOI: 10.1002/stc.127

Relationship between contact stiffness, contact depth, and mechanical properties for indentation in linear viscoelastic solids using axisymmetric indenters[‡]

Yang-Tse Cheng[1] and Che-Min Cheng[2,*,†]

[1] *Materials and Processes Laboratory, General Motors Research and Development Center, Warren, Michigan 48090, U.S.A.*
[2] *LNM, Institute of Mechanics, Chinese Academy of Sciences, Beijing 100080, China*

SUMMARY

We derive a relationship between the initial unloading slope, contact depth, and the instantaneous relaxation modulus for indentation in linear viscoelastic solids by a rigid indenter with an arbitrary axisymmetric smooth profile. Although the same expression is well known for indentation in elastic and in elastic–plastic solids, we show that it is also true for indentation in linear viscoelastic solids, provided that the unloading rate is sufficiently fast. Finite element calculations are used to illustrate the relationship for indentation using conical and spherical indenters. These results help provide a sound basis for using the relationship for determining properties of viscoelastic solids using micro- and nano-indentation techniques.

KEY WORDS: indentation; linearly viscoelastic solids; contact stiffness; contact depth; axisymmetric indenter

1. INTRODUCTION

Instrumented micro- and nano-indentation techniques are playing an important role in the study of small-scale mechanical behaviour of 'soft' matters, such as polymers, composites, biomaterials, and food products. Many of these materials exhibit viscoelastic behaviour, especially at elevated temperatures. Modelling of indentation into viscoelastic solids thus forms the basis for analysing indentation experiments in these materials. Theoretical studies of contacting linear viscoelastic bodies became active since the mid 1950s by the work of Lee [1],

*Correspondence to: C.-M. Cheng, Institute of Mechanics, Chinese Academy of Sciences, Beijing 100080, China.
† E-mail: zhengzm@lnm.imech.ac.cn
‡ This paper is written in memory of Professor Thomas Caughey who passed away suddenly last December. Che-Min recalls the memorable days with Tom at Caltech as fellow graduate students in the 1950s and Tom's hospitality during his frequent visits to Caltech in the 1980s and 1990s.

Contract/grant sponsor: NSF of China; contract/grant number: 10372101

Received 30 May 2005
Revised 6 September 2005

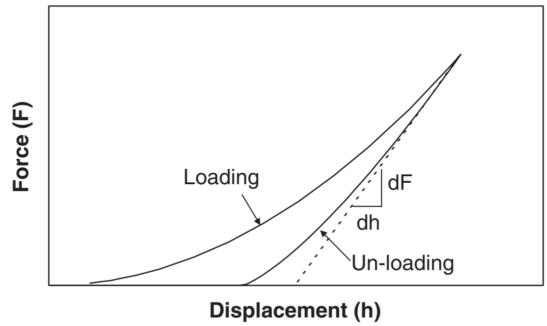

Figure 1. Typical indentation load–displacement curve and initial unloading slope.

Radok [2], Lee and Radok [3], Hunter [4], Graham [5, 6], Yang [7], and Ting [8, 9]. In recent years, a number of authors have extended the early work to the analysis of indentation measurements in viscoelastic solids [10–16].

One of the widely used approaches is to obtain the elastic modulus from the initial unloading slope (Figure 1), $\mathrm{d}F/\mathrm{d}h$, using the well-known relationship [17–21],

$$\frac{\mathrm{d}F}{\mathrm{d}h} = \frac{4G}{1-\nu}a = \frac{2E}{\sqrt{\pi}(1-\nu^2)}\sqrt{A} \tag{1}$$

where G is the shear modulus, $E = 2G/(1+\nu)$ is Young's modulus, ν is Poisson's ratio, a is the contact radius, and $A = \pi a^2$ is the contact area. Equation (1) can be derived from the theory for elastic contacts between flat surfaces and spheres [22], flat punches [22], and conical punches [23]. Furthermore, Sneddon has derived expressions for load, displacement, and contact depth for elastic contacts between a rigid, axisymmetric punch with an arbitrary smooth profile and an elastic half-space [24]. Using Sneddon's results, Pharr *et al*. [18] showed that Equation (1) holds true for rigid indenters of arbitrary smooth profiles indenting elastic solids. Equation (1) has also been applied to indentation experiments where plastic deformation occurs. Doerner and Nix [17] suggested that if the area in contact remains constant during initial unloading, the elastic behaviour might be modelled as that of a blunt punch indenting an elastic solid. Oliver *et al*. [19] pointed out that Equation (1) can be used even when the contact area between the indenter and the solid changes continuously as the indenter is withdrawn and the indenter does not behave like a flat punch. We have recently shown that Equation (1) is true for indentation in elastic–plastic solids with or without work hardening and residual stress [25]. On the other hand, Lu *et al*. [26], and Kumar and Narasimhan [27] have recently suggested that Equation (1) may not be applicable to indentation in viscoelastic solids. In this paper, we examine the validity of Equation (1) for indentation in viscoelastic solids.

2. DERIVATION

We consider a rigid, smooth, frictionless, axisymmetric indenter of arbitrary shape, $f(r)$, (Figure 2) indenting a viscoelastic solid that can be described by the following constitutive relationships

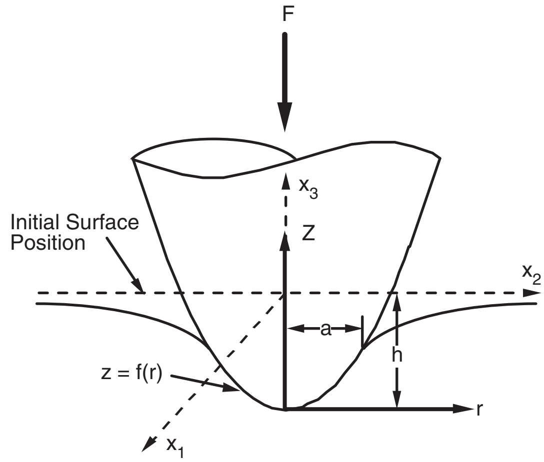

Figure 2. Illustration of surface deformation by an axisymmetric indenter.

[28, 29] between deviatoric stress and strain, s_{ij} and d_{ij}, and between dilatational stress and strain, σ_{ii} and ε_{ii},

$$s_{ij}(t) = 2\int_0^t G(t-\tau)\frac{\partial d_{ij}(\tau)}{\partial \tau}\,\mathrm{d}\tau$$

$$\sigma_{ii}(t) = 3\int_0^t K(t-\tau)\frac{\partial \varepsilon_{ii}(\tau)}{\partial \tau}\,\mathrm{d}\tau \tag{2}$$

where $G(t)$ is the relaxation modulus in shear and $K(t)$ is the relaxation modulus in dilatation. The time-dependent Young's modulus and Poisson's ratio are then given by $E(t) = [9K(t)G\times(t)]/[3K(t) + G(t)]$ and $v(t) = [E(t)/2G(t)] - 1$, respectively.

When $G(t)$, $K(t)$, and $v(t)$ are time independent, Equation (2) reduces to the ones for elastic solids. The corresponding indentation problem has been solved previously, for example by Sneddon [24], for the contact depth and indenter displacement relationship:

$$h = \int_0^1 \frac{f'(x)}{\sqrt{1-x^2}}\,\mathrm{d}x \tag{3}$$

and for the load and displacement relationship:

$$F = \frac{4Ga}{1-v}\int_0^1 \frac{x^2 f'(x)}{\sqrt{1-x^2}}\,\mathrm{d}x \tag{4}$$

where $x = r/a$. Using these relationships, Pharr *et al.* [18] derived Equation (1) for rigid indenters of arbitrary smooth profiles indenting purely elastic solids.

Applying the theories developed by Lee and Radok [3], Graham [5], and Ting [8] to the problem of indentation in viscoelastic solids and assuming time-independent

Poisson's ratio, we can write,

$$h(t) = \int_0^1 \frac{f'(x)}{\sqrt{1-x^2}}\,\mathrm{d}x \tag{5}$$

$$F(t) = \frac{4}{1-\nu}\int_0^t G(t-\tau)\frac{\mathrm{d}}{\mathrm{d}\tau}\left[a(\tau)\int_0^1 \frac{x^2 f'(x)}{\sqrt{1-x^2}}\,\mathrm{d}x\right]\mathrm{d}\tau \tag{6}$$

where $x = r/a(t)$.

Equations (5) and (6) become the familiar equations for conical indentation in linear viscoelastic solids, where $z = f(x) = (a\tan\alpha)x$ and α is the indenter half-angle. Specifically, the relationship between contact depth, $h_c(t)$, and the indenter displacement is given by, using Equation (5),

$$h(t) = \frac{\pi}{2}a(t)\tan\alpha = \frac{\pi}{2}h_c(t) \tag{7}$$

and that between force and displacement is given by, using Equation (6),

$$F(t) = \frac{4}{\pi}\frac{\cot\alpha}{(1-\nu)}\int_0^t G(t-\tau)\frac{\mathrm{d}h^2(\tau)}{\mathrm{d}\tau}\,\mathrm{d}\tau \tag{8}$$

Likewise, the equations for spherical indentation in linear viscoelastic solids, where $f(x) = \frac{1}{2}[(ax)^2/R]$ and R is the indenter radius, are given by

$$h(t) = \frac{a^2(t)}{R} = 2h_c(t) \tag{9}$$

$$F(t) = \frac{8}{3(1-\nu)R}\int_0^t G(t-\tau)\frac{\mathrm{d}a^3(\tau)}{\mathrm{d}\tau} = \frac{8\sqrt{R}}{3(1-\nu)}\int_0^t G(t-\tau)\frac{\mathrm{d}h^{3/2}(\tau)}{\mathrm{d}\tau}\,\mathrm{d}\tau \tag{10}$$

Equations (7)–(10) are special cases of more general expressions derived by Graham [5] and Ting [8]. They showed that Equations (7)–(10) are valid when the contact area is a monotonically increasing function of time. The equations for unloading where the contact area decreases monotonically have also been derived [5, 8], though they are considerably more complicated. However, we have recently demonstrated that Equations (7) and (8) and Equations (9) and (10) can be used to evaluate the initial unloading slope for conical [16,30] and spherical indentation [31] in viscoelastic solids, respectively. In the following, we use Equations (5) and (6) to derive the equation for initial unloading slopes for arbitrary indenter profiles.

Suppose unloading takes place at $t = t_m$ with a constant unloading rate of $\mathrm{d}h(t)/\mathrm{d}t|_{t_m^+} = -v_h$, we have, using Equation (6) for $0 \leqslant t \leqslant t_m + \Delta t$ and $\Delta t \to 0$,

$$\frac{F(t_m+\Delta t)-F(t_m)}{\Delta \mathrm{t}} = \frac{4}{(1-\nu)}\left\{\int_0^{t_m}\frac{\mathrm{d}G}{\mathrm{d}\eta}\bigg|_{\eta=t_m-\tau}\frac{\mathrm{d}}{\mathrm{d}\tau}\left[a(\tau)\int_0^1\frac{x^2 f'(x)}{\sqrt{1-x^2}}\,\mathrm{d}x\right]\mathrm{d}\tau\right.$$

$$\left. + G(0)\frac{\mathrm{d}}{\mathrm{d}\tau}\left[a(\tau)\int_0^1\frac{x^2 f'(x)}{\sqrt{1-x^2}}\,\mathrm{d}x\right]\right\} \tag{11}$$

Using Equation (5), the derivative in the second term on the right-hand side becomes,

$$\frac{\mathrm{d}}{\mathrm{d}\tau}a(\tau)\int_0^1 \frac{x^2 f'(x)}{\sqrt{1-x^2}}\,\mathrm{d}x = a(\tau)\frac{\mathrm{d}h(\tau)}{\mathrm{d}\tau} + \frac{\mathrm{d}a(\tau)}{\mathrm{d}\tau}h(\tau) - \frac{\mathrm{d}a(\tau)}{\mathrm{d}\tau}\int_0^1 \sqrt{1-x^2}f'(x)\,\mathrm{d}x$$

$$- a(\tau)\frac{\mathrm{d}}{\mathrm{d}\tau}\int_0^1 \sqrt{1-x^2}f'(x)\,\mathrm{d}x \qquad (12)$$

We now show that the last three terms on the right-hand side of Equation (12) cancel each other. Using $x = r/a$ and $\mathrm{d}x = \mathrm{d}r/a$, and the fundamental theorem of calculus, we obtain,

$$\frac{\mathrm{d}}{\mathrm{d}\tau}\int_0^1 \sqrt{1-x^2}\frac{\mathrm{d}f(x)}{\mathrm{d}x}\,\mathrm{d}x = \int_{r=0}^{r=a(\tau)} \frac{\partial}{\partial\tau}\left(\sqrt{1-\left(\frac{r}{a(\tau)}\right)^2}\right)\frac{\mathrm{d}f(r)}{\mathrm{d}r}\,\mathrm{d}r \qquad (13)$$

After evaluating the partial derivative in the integrand and using $x = r/a$, we have

$$\frac{\mathrm{d}}{\mathrm{d}\tau}\int_0^1 \sqrt{1-x^2}\frac{\mathrm{d}f(x)}{\mathrm{d}x}\,\mathrm{d}x = \frac{1}{a(\tau)}\frac{\mathrm{d}a(\tau)}{\mathrm{d}\tau}\left[h(\tau) - \int_0^1 \sqrt{1-x^2}\frac{\mathrm{d}f(x)}{\mathrm{d}x}\,\mathrm{d}x\right] \qquad (14)$$

Substituting Equation (14) in Equation (12),

$$\frac{\mathrm{d}}{\mathrm{d}\tau}a(\tau)\int_0^1 \frac{x^2 f'(x)}{\sqrt{1-x^2}}\,\mathrm{d}x = a(\tau)\frac{\mathrm{d}h(\tau)}{\mathrm{d}\tau} \qquad (15)$$

The initial unloading slope is then given by, using Equation (11),

$$\frac{\mathrm{d}F}{\mathrm{d}h} = \frac{\mathrm{d}F/\mathrm{d}t}{\mathrm{d}h/\mathrm{d}t} = \frac{4}{1-v}\left[G(0)a(t_m) - \frac{1}{v_h}\int_0^{t_m} \left.\frac{\mathrm{d}G}{\mathrm{d}\eta}\right|_{\eta=t_m-\tau} \frac{\mathrm{d}}{\mathrm{d}\tau}\left[a(\tau)\int_0^1 \frac{x^2 f'(x)}{\sqrt{1-x^2}}\,\mathrm{d}x\right]\mathrm{d}\tau\right] \qquad (16)$$

When the unloading rate, v_h, is sufficiently fast, the second term on the right-hand side approaches zero. Once this limiting case is reached, Equation (1) can be used to determine the 'instantaneous' moduli, $G(0)/(1-v)$ or $E(0)/(1-v^2)$, provided that the contact depth, h_c or area, A, is known as a function of $h_m = h(t_m)$. The latter condition is provided by Equation (5) for axisymmetric indenters of arbitrary profiles, which becomes Equations (7) and (9) for conical and spherical indenters, respectively.

3. FINITE ELEMENT CALCULATIONS

We now demonstrate the validity of Equations (5) and (16) for conical [16, 30] and spherical [31] indentation in linear viscoelastic solids using finite element calculations. We consider a frictionless, rigid conical indenter of half-angle $\theta = 70.3°$ indenting an isotropic linear viscoelastic solid. This indenter half-angle is chosen since its depth-to-volume relation is the same as that for the Berkovich indenter so that the results are expected to be applicable to Berkovich indentation.

A three-parameter 'standard' linear viscoelastic model is used to describe the shear and hydrostatic relaxation modulus (see Figure 3):

$$G(t) = G_1\left(1 - \frac{G_1}{G_1 + G_2}(1 - e^{-t/\tau_s})\right)$$

$$K(t) = K_1\left(1 - \frac{K_1}{K_1 + K_2}(1 - e^{-t/\tau_s})\right) \tag{17}$$

where the relaxation time $\tau_s = \eta/(G_1 + G_2)$. Various parameters are given as $G_1 = 235\,\text{MPa}$, $G_2 = 25.8\,\text{MPa}$, $K_1 = 688\,\text{MPa}$, $K_2 = 75.6\,\text{MPa}$, and $t = 0.99\,\text{s}$. The parameters are chosen such that Poisson's ratio is time independent, though both $G(t)$ and $K(t)$ are time dependent. Specifically, their values at $t = 0$ and ∞ are as follows: $G(0) = 235\,\text{MPa}$ and $G(\infty) = 23.2\,\text{MPa}$; $K(0) = 688\,\text{MPa}$ and $K(\infty) = 68.1\,\text{MPa}$; and $v = 0.483$. The parameters of this fictitious model solid are used for illustration purposes. Because of linearity, the results can be scaled to represent other materials of the same general type when the dimensionless parameters, such as G_1/G_2, K_1/K_2, G_1/K_1, and t/τ_s, are equal. Finite element calculations were carried out using the classical isotropic linear viscoelastic model implemented in ABAQUS [32] using either displacement or load as the independent variable. The finite element mesh is the same as that used in Reference [33].

For constant indentation displacement rate profiles given in Figure 4(a), the corresponding loading–unloading curves from finite element calculations are shown in Figure 4(b). These examples clearly show that, for the same loading history, the initial unloading slopes converge when unloading rate is sufficiently fast, in agreement with Equation (16). A tangent line with the converged initial unloading slope is also shown in Figure 4(b). Furthermore, Figure 4(b) suggests that the complete unloading curve converges to one limiting case as the unloading rate increases.

We next consider a frictionless, rigid spherical indenter of radius $R = 2\,\mu\text{m}$ indenting the same isotropic, three-parameter 'standard' linear viscoelastic model solid. For constant indentation displacement rate profiles given in Figure 5(a), the corresponding loading–unloading curves from finite element calculations are shown in Figure 5(b). These examples also show that, for the same loading history, the initial unloading slopes converge when unloading rate is sufficiently fast, in agreement with Equation (16).

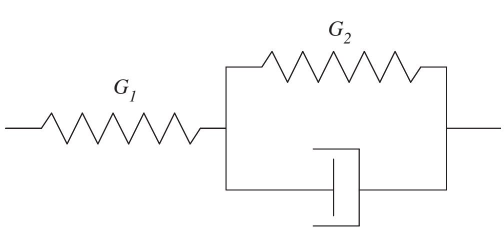

Figure 3. A three-parameter 'standard' model for linear viscoelastic solids.

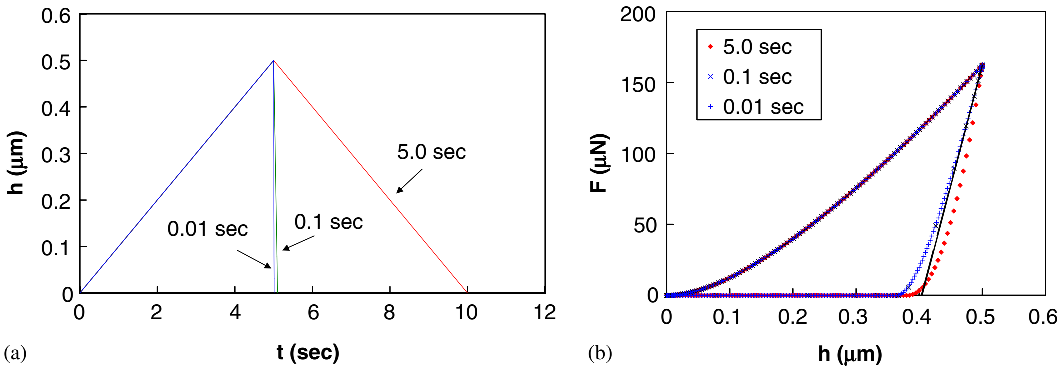

Figure 4. Conical indentation: displacement–time profiles (a) and the calculated loading–unloading curves (b) for the same loading rate and three different unloading rates. The tangent line with initial unloading slope is also shown for the converged unloading curve (b). The loading–unloading curves are labelled by the time duration of unloading.

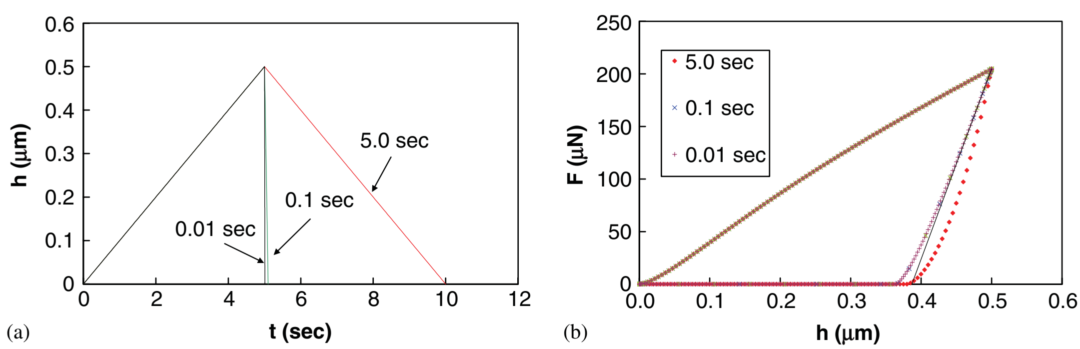

Figure 5. Spherical indentation: displacement–time profiles (a) and the calculated loading–unloading curves (b) for the same loading rate and three different unloading rates. The tangent line with initial unloading slope is also shown for the converged unloading curve (b). The loading–unloading curves are labelled by the time duration of unloading.

4. SUMMARY

We have derived a relationship between initial unloading slope, contact depth, and instantaneous relaxation modulus for indentation in linear viscoelastic solids by a rigid indenter with an arbitrary axisymmetric smooth profile. This derivation shows that with increasing unloading rate, unloading slope converges to a limiting case given by Equation (16). Thus, fast unloading is essential in determining the instantaneous modulus from the initial unloading slope using Equation (16). The relationship is demonstrated using finite element calculations for conical and spherical indenters. Presently, very little attention is paid in the literature to the unloading rate when viscoelastic properties are measured using instrumented micro- and nano-indentation techniques. This lack of attention to the unloading rate is believed to be the main cause for the reported disagreement with Equation (1). Finally, it is evident from the derivation that Equation (16) holds true for fast loading as well as for fast unloading since in both cases (i.e. $\mp v_h$) the second term in Equation (16) approaches zero. The instantaneous modulus can thus be obtained by fast jumps during either loading or unloading for indentation in linear viscoelastic solids using axisymmetric indenters of arbitrary profiles.

ACKNOWLEDGEMENTS

The authors would like to thank Wangyang Ni, Mike Lukitsch, Yue Qi, Tom Perry, and Wes Capehart, Lou Hector, and Mark W. Verbrugge for valuable discussions. C.-M. Cheng would like to acknowledge partial support from NSF of China, Project No.10372101.

REFERENCES

1. Lee EH. Stress analysis in visco-elastic bodies. *Quarterly of Applied Mathematics* 1955; **13**:183.
2. Radok JRM. Visco-elastic stress analysis. *Quarterly of Applied Mathematics* 1957; **15**:198.
3. Lee EH, Radok JRM. The contact problem for viscoelastic bodies. *Journal of Applied Mechanics* 1960; **27**:438.
4. Hunter SC. The Hertz problem for a rigid spherical indenter and a viscoelastic half-space. *Journal of the Mechanics and Physics of Solids* 1960; **8**:219.
5. Graham GAC. The contact problem in the linear theory of viscoelasticity. *International Journal of Engineering Science* 1965; **3**:27.
6. Graham GAC. The contact problem in the linear theory of viscoelasticity when the time dependent contact area has any number of maxima and minima. *International Journal of Engineering Science* 1967; **5**:495.
7. Yang WH. The contact problem for viscoelastic bodies. *Journal of Applied Mechanics* 1966; **33**:395.
8. Ting TCT. The contact stresses between a rigid indenter and a viscoelastic half-space. *Journal of Applied Mechanics* 1966; **33**:845.
9. Ting TCT. Contact problems in the linear theory of viscoelasticity. *Journal of Applied Mechanics* 1968; **35**:248.
10. Cheng L, Xia X, Yu W, Scriven LE, Gerberich WW. Flat-punch indentation of viscoelastic material. *Journal of Polymer Science*: *Part B*: *Polymer Physics* 2001; **38**:10.
11. Larrson P-L, Carlsson S. Data interpretation on microindentation of viscoelastic polymer. *Polymer Testing* 1998; **17**:49.
12. Shimizu S, Yanagimoto Y, Sakai M. Pyramidal indentation load-depth curve of viscoelastic material. *Journal of Materials Research* 1999; **14**:4075.
13. Sakai M, Shimizu S. Indentation rheometry for glass-forming materials. *Journal of Non-crystalline Solids* 2001; **282**:236.
14. Sakai M. Time-dependent viscoelastic relation between load and penetration for an axisymmteric indenter. *Philosophical Magazine A* 2002; **A82**:1841.
15. Oyen ML, Cook RF. Load-displacement behavior during sharp indentation of viscous-elastic-plastic materials. *Journal of Materials Research* 2003; **18**:139.
16. Cheng Y-T, Cheng C-M. Scaling, dimensional analysis, and indentation measurements. *Material Science and Engineering Reports* 2004; **R44**:91.
17. Doerner MF, Nix WD. A method for interpreting the data from depth-sensing indentation instruments. *Journal of Materials Research* 1986; **1**:601.
18. Pharr GM, Oliver WC, Brotzen FR. On the generality of the relationship between contact stiffness, contact area, and elastic modulus during indentation. *Journal of Materials Research* 1992; **7**:613.
19. Oliver WC, Pharr GM. An improved technique for determining hardness and elastic modulus using load and displacement sensing indentation experiments. *Journal of Materials Research* 1992; **7**:1564.
20. Briscoe BJ, Fiori L, Pelillo E. Nano-indentaion of polymeric surfaces. *Journal of Physics D*: *Applied Physics* 1998; **31**:2395.
21. VanLandingham MR. Review of instrumented indentation. *Journal of Research of the National Institute of Standard Technology* 2003; **108**:249.
22. Timoshenko SP, Goodier JN. Theory of Elasticity (3rd edn). McGraw-Hill: New York, 1970.
23. Love AE. Boussinesq's problem for a rigid cone. *Quarterly Journal of Mathematics* (*Oxford Series*) 1939; **10**:161.
24. Sneddon IN. The relation between load and penetration in the axisymmetric Boussinesq problem for a punch of arbitrary profile. *International Journal of Engineering Science* 1965; **3**:47.

25. Cheng C-M, Cheng Y-T. On the initial unloading slope in indentation of elastic-plastic solids by an indenter with an axisymmetric smooth profile. *Applied Physics Letters* 1997; **71**:2623.
26. Lu H, Wang B, Ma J, Huang G, Viswanathan H. Measurement of creep compliance of solid polymers by nanoindentation. *Mechanics of Time-Dependent Material* 2003; **7**:189.
27. Kumar MVR, Narasimhan R. Analysis of spherical indentation of linear viscoelastic materials. *Current Science* 2004; **87**:1088.
28. Findley WN, Lai JS, Onaran K. *Creep and Relaxation of Nonlinear Viscoelastic Materials*. Dover: Mineola, 1989.
29. Mase GT, Mase GE. *Continuum Mechanics for Engineers* (2nd edn). CRC: Boca Raton, 1999.
30. Cheng Y-T, Cheng C-M. Relationships between initial unloading slope, contact depth, and mechanical properties for conical indentation in linear viscoelastic solids. *Journal of Materials Research* 2005; **20**:1046.
31. Cheng Y-T, Cheng C-M. Relationships between initial unloading slope, contact depth, and mechanical properties for spherical indentation in linear viscoelastic solids. GM Research and Development Center Publication R&D – 10,059, February 21, 2005.
32. ABQUES Manual, HKS, Inc., Pawtucket, RI, U.S.A.
33. Ni W, Cheng Y-T, Cheng C-M, Grummon DS. An energy-based method for analyzing instrumented spherical indentation experiments. *Journal of Materials Research* 2004; **19**:149.